EUROMECH Young Scientist Prize Paper

"Cavitation in rubber: The role of elasticity"

Oscar Lopez Pamies won the EUROMECH Young Scientist Prize, awarded at the 7th EUROMECH SOLID Mechanics Conference held in Lisbon, September 2009

Oscar Lopez-Pamies[1]

1. Introduction

Under certain conditions, large enclosed cavities may suddenly "appear" in the interior of rubber. This phenomenon has come to be popularly known as cavitation. It corresponds, at heart, to nothing more than to the growth of defects inherent in rubber. Such defects can be of various natures (e.g., weak regions of the polymer network, actual holes, particles of dust) and of various geometries ranging from submicron to supramicron in length scale [1]. Roughly speaking, when rubber is subjected to critically large mechanical (or possibly other type of) forces, these underlying defects may suddenly grow elastically up to the point at which the surrounding polymeric chains reach their maximum elongation. Beyond that point, the defects may continue to grow inelastically by a fracture process, i.e., by the irreversible creation of new surfaces.

As a first theoretical attempt to explain and describe cavitation in rubber, Gent and Lindley [2] proposed to consider the initiation of cavitation as an *elastic instability*. In essence, they examined the elastostatics problem of a single vacuous spherical cavity of infinitesimal size (or defect) embedded at the centre of a Gaussian (i.e., Neo-Hookean) rubber ball that is subjected to uniform hydrostatic pressure on its outer boundary. Under the *faulty assumption* that rubber remains an elastic solid for arbitrarily large deformations — in other words, under the assumption that the defect can only grow elastically — they found that as the applied pressure approaches the critical value

$$P = \frac{5}{2}\mu, \tag{1}$$

where μ denotes the initial shear modulus of the rubber at zero strain, the size of the cavity suddenly becomes finite. Based on this result, Gent and Lindley [2] postulated that cavitation ensues at any point in the interior of rubber at which the hydrostatic component of the stress reaches the critical value (1). In a later effort, Ball [3] formalised and extended the result (1) to arbitrary incompressible isotropic nonlinear elastic solids (not just Neo-Hookean). This more general result reads as

1 *3106 Newmark Laboratory, University of Illinois, Urbana IL 61801-2352, pamies@illinois.edu*

$$P = \int_1^\infty \frac{1}{z^3-1}\frac{\mathrm{d}\phi}{\mathrm{d}z}\left(z^{-2}, z, z\right)\mathrm{d}z, \tag{2}$$

where $\phi = \phi(\lambda_1, \lambda_2, \lambda_3)$ stands for the stored-energy function of the solid in terms of the principal stretches $\lambda_1, \lambda_2, \lambda_3$. The unbounded upper limit of integration in (2) reveals that the onset of cavitation depends on the behaviour of the rubber at *infinitely large* deformations. While mathematically profound, this, of course, is physically incongruous since rubber behaves approximately as an elastic solid up to a critical set of large but *finite* deformations, beyond which, much like any other solid, it ruptures. Based on this observation, one might expect that the result (1), or more generally (2), is not applicable to real rubber. Yet, the result (1) has been shown by Gent and co-workers (see [1] and references therein) to agree reasonably well with a number of experimental observations. This agreement suggests that the elastic properties of rubber may play a significant — possibly even dominant — role on the onset of cavitation.

Motivated by the plausible prominence that the elastic properties of rubber may have on cavitation, Lopez-Pamies et al. [4] have recently developed a theory that permits to examine, now in full generality, the occurrence of cavitation as an elastic instability. In particular, generalizing the classical results referred to above, this new theory allows rigorous consideration of the onset of cavitation (*i*) under arbitrary loading conditions (not just hydrostatic loading), (*ii*) for general nonlinear elastic solids (not just incompressible and isotropic), and (*iii*) distributions of defects with general shapes (not just a single spherical defect). *The purpose of this paper is to test this theory using results from a classical poker-chip experiment due to Gent and Lindley [2] in order to gain insight into the relevance of the elastic properties of rubber on the phenomenon of cavitation*.

For convenience and clarity, we recall in Section 2 the elastic cavitation theory of Lopez-Pamies et al. [4] for the practically relevant case when the underlying defects at which cavitation can initiate are vacuous and their spatial distribution is random and isotropic. The specialization of this result to the basic case when the rubber is Gaussian is spelled out in Subsection 2.1. Section 3 compares this latter theoretical result with the poker-chip experiment of Gent and Lindley [2].

2. The elastic cavitation theory of Lopez-Pamies et al. [4]

Stimulated by experimental evidence [1] and the partial success of the classical theoretical results (1)-(2), Lopez-Pamies et al. [4] considered the phenomenon of cavitation in rubber as the sudden *elastic growth* of its underlying defects in response to critically large applied external loads. The defects at which cavitation can initiate were modelled as nonlinear elastic cavities of zero volume, but of arbitrary shape otherwise, that are randomly distributed throughout the rubber. This point of view led to formulating the problem of cavitation as the homogenisation problem of nonlinear elastic solids containing zero-volume cavities [6], which in turn led to the construction of a general — yet computationally tractable — rigorous criterion for the onset of cavitation.

2.1. The case of a random isotropic distribution of vacuous defects

The purpose of this paper is to test this new theory in an experiment where, due to the processing of the specimen, the spatial distribution of defects is expected to be *random* and *isotropic*. We shall further assume that the defects are *vacuous*. Granted these geometric and constitutive features for the defects, the onset-of-cavitation criterion of Lopez-Pamies et al. [4] can be stated as follows:

Inside a rubber whose nonlinear elastic response is characterized by the stored-energy function $W(\mathbf{F})$*, cavitation occurs at material points where the Cauchy stress* $\mathbf{T}$ *satisfies the condition*

$$\mathbf{T} = \frac{1}{\det \mathbf{F}} \mathbf{S}_\star(\mathbf{F})\, \mathbf{F}^T \quad \textit{with} \quad \mathbf{F} \in \partial \mathcal{Z}\left[f_\star(\mathbf{F})\right], \tag{3}$$

where $\partial \mathcal{Z}[f_\star(\mathbf{F})]$ *denotes the boundary of the zero set of* $f_\star(\mathbf{F})$*,*

$$f_\star(\mathbf{F}) \doteq \lim_{f_0 \to 0+} f(\mathbf{F}, f_0) \qquad \textit{and} \qquad \mathbf{S}_\star(\mathbf{F}) \doteq \lim_{f_0 \to 0+} \frac{\partial E}{\partial \mathbf{F}}(\mathbf{F}, f_0). \tag{4}$$

Here, the scalar functions $E(\mathbf{F}, f_0)$ *and* $f(\mathbf{F}, f_0)$ *are defined by the initial-value problems*

$$f_0 \frac{\partial E}{\partial f_0} - E - \frac{1}{4\pi} \int_{|\boldsymbol{\xi}|=1} \max_{\boldsymbol{\omega}} \left[\boldsymbol{\omega} \cdot \frac{\partial E}{\partial \mathbf{F}} \boldsymbol{\xi} - W\left(\mathbf{F} + \boldsymbol{\omega} \otimes \boldsymbol{\xi}\right) \right] \mathrm{d}\boldsymbol{\xi} = 0 \qquad \textit{with} \qquad E(\mathbf{F}, 1) = 0 \tag{5}$$

and

$$f_0 \frac{\partial f}{\partial f_0} - f - \frac{f}{4\pi} \int_{|\boldsymbol{\xi}|=1} \boldsymbol{\omega} \cdot \mathbf{F}^{-T} \boldsymbol{\xi}\, \mathrm{d}\boldsymbol{\xi} - \frac{1}{4\pi} \int_{|\boldsymbol{\xi}|=1} \boldsymbol{\omega} \cdot \frac{\partial f}{\partial \mathbf{F}} \boldsymbol{\xi}\, \mathrm{d}\boldsymbol{\xi} = 0 \qquad \textit{with} \qquad f(\mathbf{F}, 1) = 1, \tag{6}$$

where $\boldsymbol{\omega}$ *in (6) denotes the maximizing vector* $\boldsymbol{\omega}$ *in (5).*

The function E defined by the first-order nonlinear pde (5) corresponds to the total elastic energy (per unit undeformed volume) characterizing the homogenized constitutive response of a nonlinear elastic solid with stored-energy function W containing a certain isotropic distribution of disconnected vacuous cavities of initial volume fraction f_0. The function f defined by the first-order linear pde (6), on the other hand, characterizes the evolution of the volume fraction of the cavities along finite-deformation loading paths. The asymptotic behaviour (4) of these functions — in the limit as $f_0 \to 0+$ when the underlying cavities become *point defects* — are the quantities that serve to identify the critical stresses (3) at which cavitation ensues.

2.1.1. Onset of cavitation in Gaussian rubber

In the comparison with the experimental results that follows, we shall assume that the nonlinear elastic response of rubber is Gaussian (or Neo-Hookean) and thus characterised by the stored-energy function

$$W(\mathbf{F}) = \begin{cases} \frac{\mu}{2}[\mathbf{F} \cdot \mathbf{F} - 3] & \text{if } \det \mathbf{F} = 1 \\ +\infty & \text{otherwise} \end{cases}, \tag{7}$$

where, again, μ stands for the initial shear modulus of the specific rubber under investigation. For this type of behaviour, the limiting functions (4) can be shown to be given by

$$f_\star(\mathbf{F}) = 1 - \frac{1}{\det \mathbf{F}} \qquad \text{and} \qquad \mathbf{S}_\star(\mathbf{F}) = \mu \mathbf{F} + \frac{\mu(1 + 2 \det \mathbf{F})}{2(\det \mathbf{F})^{1/3}} \Phi(\mathbf{F})\, \mathbf{F}^{-T} + \frac{3\mu(\det \mathbf{F} - 1)}{2(\det \mathbf{F})^{1/3}} \frac{\partial \Phi}{\partial \mathbf{F}}(\mathbf{F}), \tag{8}$$

where the function Φ is defined implicitly by a first-order nonlinear pde in two variables (see Section 3.1 and Appendix C in [7]). For all practical purposes, as discussed in Section 6 of [7], the function Φ may be approximated simply as being equal to its maximum value, $\Phi = 1$. By making use of this approximation, it is not difficult to deduce that the cavitation criterion (3)-(6) reduces in this case to:

$$8 t_1 t_2 t_3 - 12\mu(t_1 t_2 + t_2 t_3 + t_3 t_1) + 18\mu^2(t_1 + t_2 + t_3) - 35\mu^3 = 0 \quad \textit{with} \quad t_i > \frac{3}{2}\mu. \tag{9}$$

The interested reader is referred to [7] for the derivation and thorough discussion of the criterion (9). Here, it is relevant to record that for states of purely dilatational stress when $t_1 = t_2 = t_3 = P$, the general criterion (6) reduces — rather remarkably, as explained in Section 5 of [4] — to the approximate "hydrostatic" criterion proposed by Gent and Lindley [2]:

$$\frac{1}{3}(t_1 + t_2 + t_3) - \frac{5}{2}\mu = 0. \tag{10}$$

For more complex states of stress with non-vanishing shear ($t_2 - t_1 = 0$ and/or $t_3 - t_1 = 0$), the general criterion (9) — as opposed to the hydrostatic criterion (10) — indicates that cavitation occurs at mean stress values $P = (t_1 + t_2 + t_3)/3 > 5/2\mu$. In other words, shear stresses stabilize the rubber in the sense that their presence postpones the onset of cavitation.

3. Comparison of the theory with the poker-chip experiments of Gent and Lindley [2]

In a seminal contribution, Gent and Lindley [2] reported a beautiful set of experiments where cavitation was induced within thin disks of rubber bonded to metal plates subjected to uniaxial tensile forces. Specifically, the test-pieces were made up of thin disks of (filled and unfilled) natural rubber bonded to circular metallic plates by means of cement during the vulcanisation process. The rubber disks were $R = 1$ cm in initial radius and from $H = 0.056$ cm to $H = 0.980$ cm in initial thickness (hence their name "poker-chip" experiments). The load was applied quasistatically under displacement control by means of a Hounsfield tensometer, which provided

measurements of the load f induced by a given applied displacement $h - H$. Gent and Lindley [2] reported these raw measurements in terms of the "macroscopic" stress measure $\sigma = \mathrm{f}/\pi R^2$ and the "macroscopic" strain measure $\varepsilon = h/H - 1$. Figure 1 depicts a schematic of the geometry and deformation of the specimens with the various quantities of interest indicated.

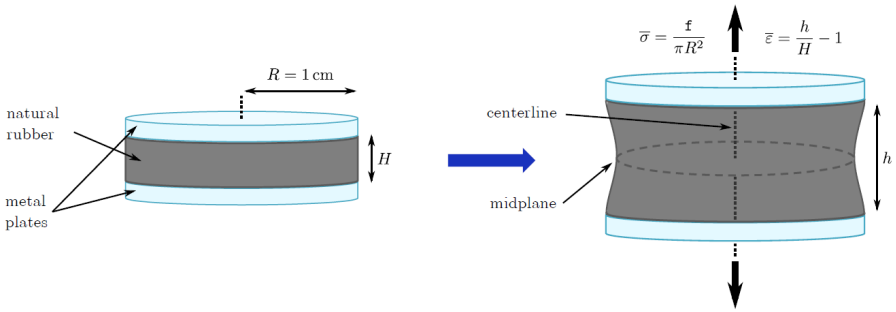

Fig. 1 Schematic of the poker-chip experimental setup of Gent and Lindley [2]. The initial radius of the rubber disks was fixed at R = 1 cm, while their initial thicknesses were varied from H = 0.056 cm to H = 0.980 cm in order to induce stress fields with a wide range of triaxialities (from large for the thinnest disk to relatively small for the thickest one) inside the rubber.

In the sequel, we report finite-element (FE) simulations of the experiment of Gent and Lindley [2] for the thinnest rubber disk with $H = 0.056$ cm. We begin in Subsection 3.1 by showing when and where the cavitation criterion (9) is satisfied within the disk, as a function of the applied macroscopic strain ε. In Subsection 3.2, we explicitly introduce defects — in the form of vacuous spherical cavities of $\Delta = 1\ \mu\mathrm{m}$ radius —into the FE model at the locations disclosed by the criterion, in order to investigate the ensuing growth and interaction of the "nucleated" cavities upon further loading. We dedicate Subsection 3.3 to comparing the simulations with the experiment.

3.1. Pointwise monitoring of the cavitation criterion

Figure 2 shows the deformed configurations of the rubber disk with thickness $H = 0.056$ cm at five values of the applied macroscopic strain, $\varepsilon = 0,\ 0.2816,\ 0.2820,\ 0.2998$, and 1.40%. Material points at which the cavitation criterion (9) is satisfied are depicted in red.

As indicated by arrows in Fig. 2(b), the first points to reach the cavitation criterion are those at the rubber/plates interfaces along the centreline of the disk. This is because — in contrast to popular belief in the literature — the hydrostatic stress in poker-chip experiments is always largest at the rubber/plates interfaces along the centreline of the test-piece, and *not* at the centre of the rubber disk. As the applied strain ε increases, the region where the criterion is satisfied grows radially along the rubber/plates interfaces and also propagates to the centre of the rubber disk reaching it at the value $\varepsilon = 0.2820\%$; this is shown by Fig. 2(c). As the applied strain ε increases even further, the region where the criterion is satisfied continues to grow radially from the centreline of the disk towards its lateral free boundary. Figures 2(d) and (e) illustrate two snapshots of this propagation.

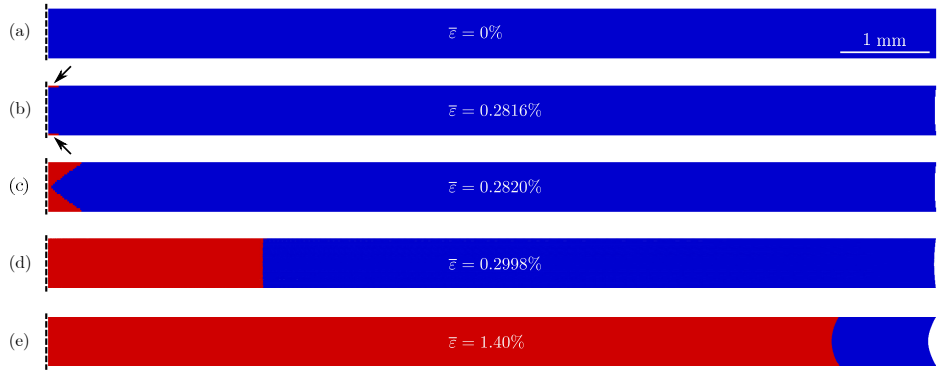

Fig. 2 Axisymmetric FE simulation of the poker-chip experiment with rubber disk thickness H = 0.056 cm. Parts (a) through (e) show the deformed configurations of half (for better visualization) of the rubber disk at five values of the applied macroscopic strain ◘. The material points at which the cavitation criterion (9) is progressively satisfied are depicted in red.

3.2. Full-field simulations accounting for the growth of the defects

The preceding analysis has served to reveal the critical macroscopic loads and associated spatial locations at which defects in rubber may start to grow to finite sizes during poker-chip experiments (with thin rubber disks). In this subsection, we investigate the extent to which they grow and how they interact with one another. To this end, we introduce defects explicitly in the FE models at the locations disclosed by the criterion (9) and monitor their growth. Here, defects are modelled as vacuous spherical cavities of initial radius $\Delta = 1\ \mu\mathrm{m}$. In this regard, it is important to remark that we have performed a variety of simulations wherein the defects are micron and submicron in size and spherical and non-spherical in shape. Interestingly, the results of such simulations indicate that provided the defects are no larger than roughly $1\ \mu\mathrm{m}$ in length scale, their specific shape and size do not significantly influence when and how they grow (at

least during the poker-chip simulations of interest here), hence our choice to model them as spherical cavities of initial radius $\Delta = 1\ \mu\mathrm{m}$.

For sufficiently thin test-pieces such as the one considered here, the attainability of the cavitation criterion (9) eventually propagates across the larger part of the rubber disk. In the sequel, we thus consider the explicit presence of defects throughout the rubber. Because of the extremely small size of the defects ($1\ \mu\mathrm{m}$ in radius), the discretisation of the rubber disk explicitly containing defects is required to be in the form of a structured mesh. In practice, this requirement forces the spatial distribution of defects in the simulations to exhibit some level of periodicity thus preventing the consideration of a truly random distribution. For definiteness, based on results from a variety of distributions [5], we consider here that the defects are located within three planes: a plane adjacent ($1\ \mu\mathrm{m}$ away) to the top rubber/plate interface, a plane adjacent ($1\ \mu\mathrm{m}$ away) to the bottom rubber/plate interface, and the midplane of the rubber disk. Within each of these planes, 5 defects at radial distances 0, 0.25, 0.50, 0.75, and $0.95\ \mathrm{cm}$ from their centre are placed at angular intervals of $\pi/8$ radians. This amounts to a total of 65 defects per plane, and thus a total of 195 defects in the entire rubber disk.

Figures 3(a) through (d) depict a 2D radial perspective of half of the disk at various values of the applied macroscopic strain, $\varepsilon = 0$, 0.43, 1.00, and 2.30%. This string of snapshots show that the first defect to grow is the one located in the centre of the disk and that, upon further loading, adjacent midplane defects successively grow in a radial cascading sequence; as the exception, the defects closest to the lateral free boundary of the disk do not grow. This seemingly intricate behaviour can be readily understood from an energetic standpoint. Indeed, even though the cavitation criterion (9) is first satisfied at the rubber/plates interfaces slightly before than at the centre of the disk (see Fig. 2), it is energetically more favourable for the defect at the centre to accommodate all of the initial growth. As the macroscopic strain ε increases and satisfaction of the criterion (9) propagates radially outwards (see Fig. 2), it becomes energetically more favourable for the defects in the midplane of the disk adjacent to its centre — and *not* those near the rubber/plates interfaces — to then accommodate most of the growth at the expense of the defect at the centre. This radial cascading trend continues across the disk for increasing strains all the way up to reaching a narrow region containing the lateral boundary of the disk. There, the state of stress does not satisfy the criterion (9) and hence the underlying defects do not grow.

To aid the quantitative understanding of the above-described growth and interaction of defects and also their effect on the overall mechanical response of the poker-chip test-piece, Figs. 3(e) and (f) show plots of the volume variation v/V of the midplane defects and of the normalized macroscopic stress σ/μ as functions of ε. Figure 3(e) distinctly illustrates the radial cascading nature of the growth of the midplane defects with increasing loading. The primary observation from Fig. 3(f) is that the growth of midplane defects entails a severe softening of the overall mechanical response of the rubber disk; the response of the perfect rubber disk without defects is plotted in the same figure for direct comparison. Since the rubber is assumed to remain elastic for arbitrarily large deformations, this softening is purely *geometrical* in nature.

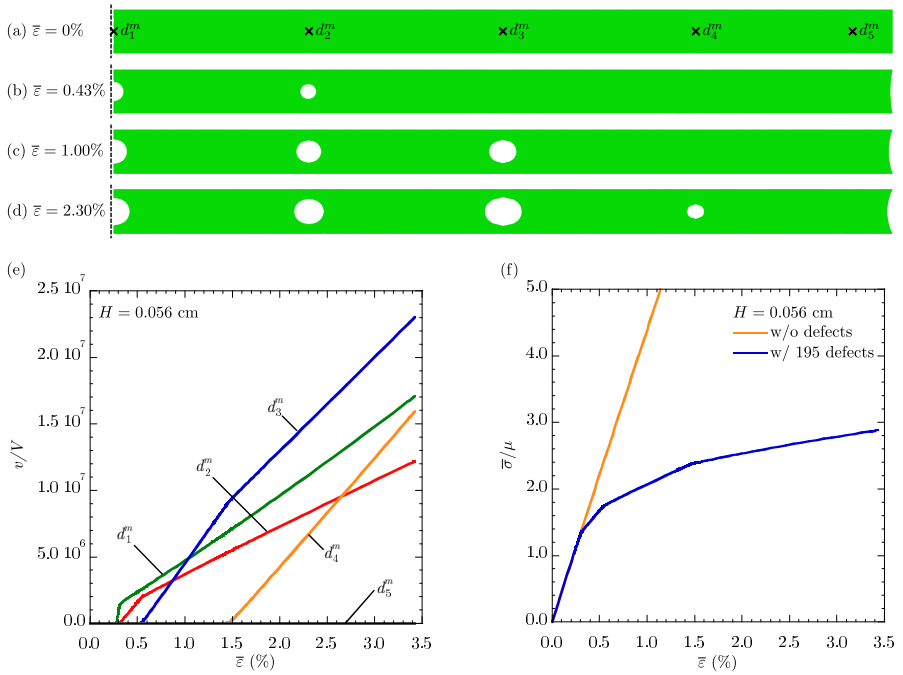

Fig. 3 3D FE simulation of the poker-chip experiment with rubber disk thickness H = 0.056 cm containing 195 defects throughout the entire disk. Parts (a) through (d) show a 2D radial perspective of half of the rubber disk at four values of the applied macroscopic strain ε. Parts (e) and (f) show plots of the volume variation of the midplane defects and the normalized macroscopic stress σ/μ as functions of ε.

3.3. Elastic cavitation theory vs. experiments

We are now in a position to apply the foregoing theoretical results to the experimental observations and measurements of Gent and Lindley [2]. Figure 4 reproduces a photograph of the midplane of a test-piece, made up of natural rubber with disk thickness $H = 0.061\ \mathrm{cm}$, cut open after being subjected to a macroscopic stress of $\sigma = 2.74$ MPa; the shear modulus of the rubber is

$\mu = 0.59$ MPa (labelled as vulcanisate D in [2]). A key observation from this figure is that cavities appear in the midplane of the disk and *not* elsewhere. Another key observation is that cavities appear pervasively over the entire midplane, with the exception of a narrow region around the lateral free boundary. Remarkably, these two features are in agreement with the simulations, even though, again, the simulations assume that the rubber is Gaussian and that the defects can only grow elastically. This, of course, is not the case in the experiment. Indeed, the natural rubber utilized in the experiment is comprised of polymeric chains of finite length and thus its behaviour is not Gaussian beyond moderately large deformations (typically of the order of 300%). Moreover, as plainly shown by the post-mortem snapshot in Fig. 4, the defects do grow inelastically by the irreversible creation of new surface.

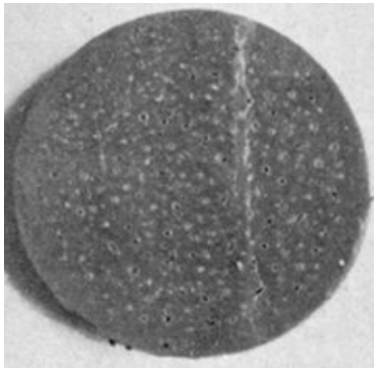

Fig. 4 Midplane of a poker-chip test-piece with disk thickness H = 0.061 cm, made up of natural rubber with initial shear modulus $\mu = 0.59$ MPa, cut open after being subjected to a macroscopic stress of $\sigma = 2.74$ MPa [2].

While Gent and Lindley [2] did not monitor the growth of the defects *in-situ* (other than crudely in one of their specimens made up of transparent rubber, vulcanisate G), more recent poker-chip experiments have made use of X-ray computer tomography to access such information [8]. These experiments have shown that the cavities appear first in the centre of the disk and subsequently downstream in the direction of the lateral boundary. This radial cascading sequence is also in agreement with the simulations.

The comparisons presented in this paper (together with the more comprehensive results to be reported in [5]) have shown that theoretical results based on the premise that rubber is Gaussian and the further assumption that its inherent defects are vacuous and isotropically distributed are in good *qualitative* agreement with experiments in the sense of: (*i*) when and where cavitation first occurs as well as (*ii*) how cavities continue to grow and interact once they have been "nucleated". This remarkable agreement suggests that the sudden growth of defects and their ensuing behaviour and interaction with other defects in real rubber is driven predominantly by the minimization of the elastic energy of the rubber. A direct practical implication of such a prominence of the elastic properties is that the *elastic* criterion (9) can be utilized effectively to gain quick insight into the possible occurrence of cavitation in real material systems comprising rubber.

4. References

[1] Gent, A.N., 1991.Cavitation in rubber: a cautionary tale. *Rubber Chem. Technol.* 63, G49–G53.

[2] Gent, A.N., Lindley, P.B., 1959. Internal rupture of bonded rubber cylinders in tension. *Proceedings of the Royal Society A* 2, 195–205.

[3] Ball, J.M., 1982. Discontinuous equilibrium solutions and cavitation in nonlinear elasticity. *Philosophical Transactions of the Royal Society of London A* 306, 557–610.

[4] Lopez-Pamies, O., Idiart, M.I., Nakamura, T. 2011. Cavitation in elastomeric solids: I — A defect-growth theory. *Journal of the Mechanics and Physics of Solids* 59, 1464–1487.

[5] Lefèvre, V., Ravi-Chandar, K., Lopez-Pamies, O. 2014. Cavitation in rubber: An elastic instability or a fracture phenomenon?. In preparation.

[6] Lopez-Pamies, O., 2009. Onset of cavitation in compressible, isotropic, hyperelastic solids. *J. Elast.* 94, 115–145.

[7] Lopez-Pamies, O., Nakamura, T., Idiart, M.I. 2011. Cavitation in elastomeric solids: II — Onset-of-cavitation surfaces for Neo-Hookean materials. *Journal of the Mechanics and Physics of Solids* 59, 1488–1505.

[8] Bayraktar, E., Bessri, K., Bathias, C. 2008. Deformation behaviour of elastomeric matrix composites under static loading conditions. *Eng. Fract. Mech.*75, 2695–2706.